Theoretical and Experimental Investigation on the Characteristics of Fly-Ash Scrubbing in a Fixed Valve Tray Column

Qingli Wang, Xueli Chen, and Xin Gong
Key Laboratory of Coal Gasification and Energy Chemical Engineering of Ministry of Education, East China University of Science and Technology, Shanghai 200237, PR. China

DOI 10.1002/aic.13967
Published online December 7, 2012 in Wiley Online Library (wileyonlinelibrary.com).

The goal of this study is to evaluate the performance of a fixed valve tray column designed to remove fly-ash particles. A series of experiments were carried out at room temperature to demonstrate the collection efficiency of a fixed valve tray column at different gas and liquid superficial velocities. The fly-ash particles removal characteristics of the fixed valve tray column were evaluated by measuring variations of concentration and size distribution of particles in the outlet. The mechanism of particle removal in this turbulent dispersion system was theoretically analyzed on the basis of diffusion, interception, sedimentation and impaction, and a model was proposed to predict the collection efficiency. The results show that the simulation results agree well with the experimental data. In contrast to most of the conventional models, the present model is capable of evaluating the effects of bubble hydrodynamics, system property, and operation conditions on the collection efficiency. The model is expected to guide effectively the design and operation of valve tray washing columns, which is widely applied nowadays. © 2012 American Institute of Chemical Engineers *AIChE J,* 59: 2168–2178, 2013
Keywords: coal gasification fly-ash, fixed valve tray, particle collection efficiency, bubble scrubber, tray column

Introduction

A coal-fired power plant releases large amounts of pollutants, such as particulates, SO_X, and NO_X, into the atmosphere. Air quality can be safeguarded only by effectively reducing the emission of these types of pollutants. Integrated gasification combined cycle (IGCC) is an important method that has been applied in advanced coal-fired power generation plants since the 1970s.

In IGCC systems, the particulate cleanup process plays an important role in the whole system. It removes the particles from syngas produced in the gasifier before the syngas enters the gas turbine, and this is necessary as for protect the turbine blades and for control particulate emissions. It is important to incorporate methods for particulate cleanup for the optimization of IGCC systems. Unlike the syngas purification in GE gasification technology, in the opposed multiburner (OMB) gasification purification process, a combination of mixer, cyclone, and washing column is adopted.[1] Cyclones are very effective in removing relatively large particles from a gas stream. However, their particle collection efficiency rapidly decreases with decreasing particle size,[2,3] so washing column is adopted for the deeper purification of syngas, the goal is to control the concentration of particles below 1 mg/(N m^3) in syngas.[4]

In general, conventional wet scrubbers often suffer from clogging and fouling problems by salt formation at the tip, the inside and outside of the nozzles, the tubes, and the walls of scrubbers. Another drawback is the conventional scrubbers usually depend more on some form of inertial as the primary mechanism of capture. Unfortunately, inertial forces become insignificantly small as particle size decreases, and collection efficiency decreases rapidly as particle size decreases. As a result, it becomes necessary to greatly increase the energy input to a wet scrubber to significantly improve collection efficiency of fine particles.[5] Bubble column is very suitable to remove tiny particles from the gas. However, the efficiency in a normal bubble column is very limited, due to the limitations of specific interfacial area α.[6,7] In addition, large amount of energy is to be consumed for generating small bubbles. Thus, the mass-transfer efficiency of single-stage bubble column cannot be very high. To achieve high efficiency of mass transfer, bubble columns must be operated in series or in multiple stages.[8] However; there were very limited studies on scrubbing of particles in stage bubble column scrubber. Many of the processes reported have been covered by patent protections.[9,10]

Tray column is widely used in air pollution control and gas–solid separation for aerosol sampling and industrial applications. The large surface-to-volume ratio and low-pressure drop of such a system, combined with the fact that when bubble is broken, the particulates are concentrated into a small volume, make the process promising.[11,12] Local characteristics of gas–liquid flows and particle properties are two main factors affecting collection efficiency in fixed valve columns. In these system, liquid is in the form of small bubbles, so that the gas–liquid interfacial area is very large,

Correspondence concerning this article should be addressed to X. Chen at cxl@ecust.edu.cn.

with this tremendous cleaning area available, the particle travels only a very short distance before colliding with a liquid cleaning surface. These conditions are ideal for promotion of rapid separation. The mechanisms by which particulates are collected by bubbles include interception, inertial impaction, diffusion, gravitational sedimentation, and electrostatic attraction. Fuchs[13] was the first to attempt a theoretical explanation for the experimental observations of pool scrubbing of particles. He derived the particle removal efficiencies due to Brownian diffusion, inertial impaction, and gravitational sedimentation by assuming that particles are homogeneously distributed in each bubble. According to Kaldor et al.,[11] gravitational sedimentation is the predominant mechanism. Nevertheless, diffusion also plays an important role in capturing submicron-sized particulates. Lee and Gieseke[14] obtained the particle collection efficiencies due to Brownian diffusion and interception using the flow field of Kuwabara's cell model. Later, Jung and Lee[15] extended the flow field of Kuwabara's cell model to treat the flow field around multiple liquid droplets or gas bubbles by taking into account the effects of the internal circulation inside the droplets or bubbles on the outside flow field and on the particle collection efficiency. The particle removing efficiencies due to Brownian diffusion and interception are considered. In recent years, Mohan[16] reported a systematic mathematical approach on the basis of Kim's theory as well as detailed experimental studies on the removal of dust particles from hot gases using a spray column. Park and Lee[17,18] developed a novel aerosol filtering device, the swirl cyclone scrubber that mainly consists of a cyclone and a swirl scrubber and derived the model of particle collection efficiency due to Brownian diffusion, inertial impaction, and gravitational sedimentation on the basis of Fuchs theory. However, there are none of theoretical models that are especially applicable to the tray columns. Therefore, the main objective of this work is to analyze the functioning mechanism of bubble hydrodynamics, system property, and operation conditions on the collection efficiency and derive an appropriate correlation. The model would be limited to crossflow fixed valve trays but might have possible extensions to other crossflow devices such as bubble-cap trays and sieve trays.

Mechanism of Particle Collection

When particle-laden gas passes up through a water layer on the tray, a number of small air bubbles are formed. In a process called bubble scrubbing, fly-ash particles entrained in bubbles rising through the gas–water mixture on the tray were collected on the bubble surface due to various transport mechanisms including Brownian diffusion, interception, gravitational sedimentation, and inertial impaction. Figure 1 illustrates the principle of particle collection in a rising bubble. Normally, when the particle size is less than 0.1 μm, Brownian diffusion becomes significant (Particle 1).[11] When particles larger than 5.0 μm, inertial impaction remains an important mechanism, and in this case, a particle carried along by an air stream on approaching an obstruction tends to follow the stream but may strike the obstruction because of its inertia (Particle 2). Interception, even if the trajectory of a particle does not depart from the streamline, a particle may still be collected when the particle passes within one particle radius from the bubble surface (Particle 3).[13] In the case of gravitational sedimentation, particles in a slowly moving air stream may settle out on the collecting surface under the influence of gravity (Particle 4). If significant evaporation or condensation takes place, Stefan flow can impose an additional aerodynamic impact on the motion of particles (Particle 5).[15] In this study, this effect is neglected. Thus, a fundamental analysis of the impaction process must also include an analysis of the various mechanisms of impaction and collection.

Theoretical Modeling of Collection Efficiency in Washing Column

Basic assumptions

The following major assumptions are made in developing the proposed model to study the prediction for performance of the fixed valve tray column:

1 No loading occurs on the bubbles, and the particles adhere to the bubbles surface on contact.

2 No coalescence occurs between the bubbles.

3 Gas follows ideal gas law.

4 Bubbles are spherical.

5 Particle size distribution is uniform, and bubble sizes are same.

Mass balance equation

A mathematical model based on mass balance has been developed over a control volume of the fixed valve column. Applying mass balance equation to a cylindrical element of height dz taken inside the fixed valve column as shown in Figure 2, we obtain the following equation

$$\text{particle flux from gas to liquid} = \text{particle flux into gas-liquid mixture} - \text{particle flux of penetration}$$

In bubble scrubbing process, fly-ash particles entrained in air bubbles rising through the gas-liquid were collected on the bubble surface due to various transport mechanisms. So, particle flux from gas to liquid can be written as follows

$$\begin{aligned}\text{particle flux from gas to liquid} &= \text{swept volume of moving bubbles} \times \text{particle concentration in bubble} \times \text{fraction of particles collect in a bubble swept vlome of moving bubbles}\\ &= \text{number of bubbles swept} \times \text{bubble residence time} \times \text{volumetric flux}\end{aligned}$$

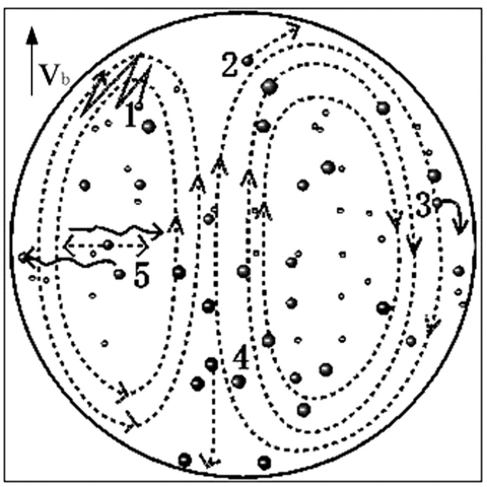

Figure 1. Particle removal mechanisms in a rising bubble.

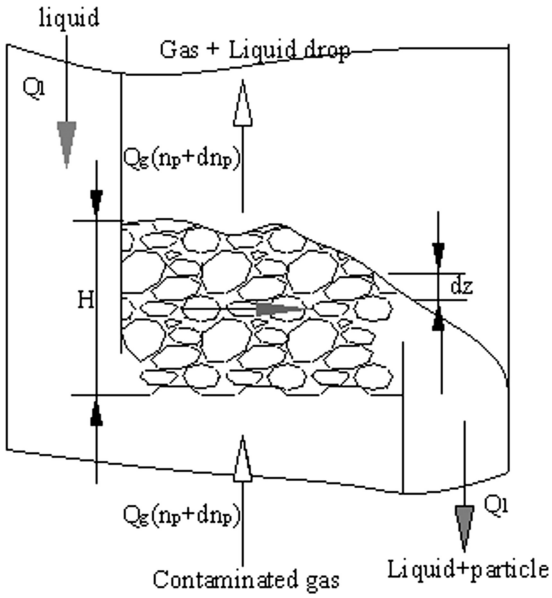

Figure 2. Schematic of fixed valve tray column.

Therefore, mass balance equation can be rewritten as Eq. 1

$$-\frac{Q_G}{A_c}dc = \frac{6Q_G}{\pi d_b^3 A_c}\cdot\frac{dz}{v_b}\cdot\frac{\pi d_b^2}{4}\cdot U\cdot c\cdot\eta_s \tag{1}$$

where Q_G is the gas flow rate (m^3/s), Q_L, the liquid flow rate (m^3/s), A_c, tray bubbling area (m^2), U, the relative velocity between bubbles and liquid (m/s), c, the particle concentration in bubble (g/m^3), η_s, the fraction of particles collected in a bubble, d_b, the Sauter bubble mean diameter (m), and v_b, the bubble velocity (m/s).

Equation 2 is derived using Eq. 1 and can be integrated over the mean effective height of gas–liquid mixture on the tray, H_F, to yield Eq. 3.

$$\frac{dc}{dz} = -\frac{3}{2}\cdot\eta_s\cdot\frac{U}{d_b v_b}\cdot c \tag{2}$$

$$\frac{c}{c_0} = \exp\left\{-\frac{3}{2}\cdot\eta_s\cdot\frac{U}{v_b}\cdot\frac{H_F}{d_b}\right\} \tag{3}$$

Hence

$$\eta_{total} = 1-\frac{c}{c_0} = 1-\exp\left\{-\frac{3}{2}\cdot\frac{U}{v_b}\cdot\frac{H_F}{d_b}\cdot\eta_s\right\} \tag{4}$$

Gas holdup in fixed valve tray column

Gas holdup, one of the most important parameters, has been involved in many research articles, and it is mainly affected by the tray geometry and gas velocity. In this work, the clear liquid height and froth height were experimentally determined to calculate gas holdup using the following expression[19,20]

$$\varphi_g = (H_F - H_0)/H_F \tag{5}$$

where φ_g is the gas holdup, H_0 the clear liquid height, and H_F the froth height.

Bubble size and velocity in fixed valve tray column

In turbulent flow of liquid containing dispersed bubbles, breakup and coalescence usually take place continuously and these processes determine the bubble size distribution. The fundamental work in dispersion theory in turbulent flow was conducted independently by both Kolmogoroff[21] and Hinze.[22] They postulated that most of the turbulent energy is dissipated by these small eddies; a part of the turbulent energy may be converted to heat energy through viscous dissipation, whereas the other part may contribute to surface energy during the bubble deformation.

As the fundamental contributions by Kolmogoroff and Hinze, bubble breakup in the inertial subrange of locally isotropic turbulence has been extensively studied by many, including Levich,[23] Sevik and Park,[24] Hesketh and Russell,[25] Wilkinson et al.,[26] Martinez-Bazan et al.,[27,28] and Risso.[29] The general understanding is that the turbulent breakage is induced by eddies bombarding and deforming the bubble surface. Only a certain number of bubble-eddy collisions are likely to result in bubble crushing, and the break up of bubbles is determined by the equilibrium between the inertial force of the arriving eddy F_λ and the interfacial force F_σ. The balance of disruptive and cohesive forces is generally expressed in terms of the dimensionless Weber number. A critical Weber number We_c will exist at the point where cohesive and disruptive forces become balanced under a maximum stable bubble size d_{max}.

$$We_c = F_\lambda/F_\sigma = \overline{u^2}\rho_L d_{max}\Big/\sigma \tag{6}$$

The mean-square spatial fluctuating velocity term, $\overline{u^2}$, describes the turbulent pressure forces of eddies of size d and is defined as the average of the square of the differences in velocity over a distance equal to the bubble diameter. In isotropic homogenous turbulence, this velocity term is a function of the energy dissipation rate per unit mass, ε. Batchelor[30] derives this relationship as

$$\overline{u^2} = 2(\varepsilon d_{max})^{2/3} \tag{7}$$

Combining critical Weber number with Eq. 7 results in the following equation for d_{max}

$$d_{max} = \left(\frac{We_c}{2}\right)^{3/5}\left(\frac{\sigma}{\rho_L}\right)^{3/5}\varepsilon^{-2/5} \tag{8}$$

This equation describes the maximum bubble size as a function of the local energy dissipated by the turbulence and the physical properties of the fluids. In a fixed valve tray column, the local energy dissipation rate per unit mass, ε, can be expressed as

$$\varepsilon = C_d\cdot u_G\cdot g \tag{9}$$

where $0 < C_d < 1$ is the percentage of energy dissipation that is dependent on the tray configurations, u_g the superficial gas velocity. C_d has different values for various fixed valve geometries, despite the fact that for all kinds of valve trays the gas jets out from valve slots.[31]

Meanwhile, average bubble size is of more importance than d_{max} in the industrial applications, as the former is based on

the size distribution of all bubbles and generally obtained by the method of statistical averaging, rather than a single measurement. The most important statistical measurement reported in the literature is the Sauter mean bubble diameter, d_b, that indicates the ratio of bubble volume to the surface area for a sample of N bubbles and is defined as follows

$$d_b = \frac{\sum_{i=1}^{N} d_i^3}{\sum_{i=1}^{N} d_i^2} \tag{10}$$

Hesketh and Russell[25] assumed that these bubble size data fit a log normal distribution. Thus, the coefficient between d_b and d_{max} could be expressed as a function of geometric mean standard deviation

$$C_n = d_b/d_{max} = \exp(2.5 \ln^2 \sigma_g - 2.33 \ln \sigma_g) \tag{11}$$

The average value of the coefficient is approximately a constant ($C_n = 0.62$) for a wide range of systems.

For the valve tray, the actual d_b is expressed by inducing Eqs. 8 and 9 into Eq. 11

$$d_b = \frac{C_n}{C_d^{2/5}} \cdot \left(\frac{We_c}{2}\right)^{3/5} \cdot \left(\frac{\sigma}{\rho_L}\right)^{3/5} (u_g g)^{-2/5} \tag{12}$$

Equation 12 is substituted into Eq. 4

$$\eta_{total} = 1 - \frac{c}{c_0} = 1 - \exp\left\{-\frac{3}{2} \cdot \beta \cdot (u_g g)^{2/5} \cdot \left(\frac{\sigma}{\rho_L}\right)^{-3/5} \cdot \frac{U}{v_b} \cdot H_F \cdot \eta_s\right\} \tag{13}$$

$$\beta = \frac{C_d^{2/5}}{C_n} \cdot \left(\frac{We_c}{2}\right)^{-3/5} \tag{14}$$

Although the velocity of any individual bubble in the dispersion cannot be predicted with any certainty, the mean velocity of a sample of many bubbles of a given size is a reproducible quantity that is significantly related to the bubble superficial gas velocity and gas holdup. The bubble slip velocity is calculated from the following relationship[32]

$$v_b = u_g/\varphi_g - u_l/\varphi_l \tag{15}$$

The fraction of particles collected in a bubble

The fraction of particles collected in a bubble using one or more of several collection mechanisms, such as impaction, interception, diffusion, electrostatic attraction, condensation, centrifugal force, and gravity. However, diffusion, interception, impaction, and gravitational sedimentation are the four primary ones in bubble columns.[13–15] The theoretical equations were used for predicting the single bubble efficiency by considering all the four mechanisms. Particle collection by diffusion mechanism is dominant for submicron particle size in bubble scrubbers. Small particles attain a high diffusion coefficient, because the diffusion coefficient is inversely proportional to size. The diffusive collection efficiency of a single bubble is given by Fuchs.[13]

$$\eta_{diff} = 3.6\left(\frac{2}{d_b^2}\right)^{\frac{1}{2}} Pe^{-\frac{1}{2}} \tag{16}$$

$$Pe = \frac{d_b v_b}{D_{diff}} \tag{17}$$

where Pe is the Peclet number. For the diffusion coefficient, D_{diff}, appearing in the Peclet number, the following form is used[33]

$$D_{diff} = \frac{kTC}{3\pi\mu d_p} \tag{18}$$

where k is the Boltzmann constant, T, the absolute temperature, μ, the viscosity of the air, d_p, the particle diameter, and C, the Cunningham slip correction factor. Here, the value of C is obtained by the following equation[34]

$$C = 1 + 2.284\frac{\lambda}{d_p} + 1.116\frac{\lambda}{d_p}\exp\left(-0.4995\frac{\lambda}{d_p}\right) \tag{19}$$

where λ is the mean free path length of molecule.

Even if the trajectory of a particle does not depart from the streamline, a particle may still be collected when the particle passes within one particle radius from the bubble surface. This phenomenon is known as interception mechanism of particle removal. The dimensionless parameter describing the interception effect, R, is defined as the ratio of particle diameter to bubble diameter, as shown

$$R = \frac{d_p}{d_b} \tag{20}$$

Jung and Lee[15] derived the following collection efficiency of a bubble due to interception mechanism

$$\eta_{int} = \left(\frac{1-\varphi_g}{J}\right)\left\{\left(\frac{R}{1+R}\right) + 2\left(\frac{R}{1+R}\right)^2\right\} \tag{21}$$

$$J = 1 - \frac{6}{5}\varphi_g^{1/3} + \frac{1}{5}\varphi_g^2 \tag{22}$$

Rearranging for R

$$\eta_{int} = \left(\frac{1-\varphi_g}{J}\right)(R + 2R^2) = \left(\frac{1-\varphi_g}{J} \cdot \frac{1}{d_b}\right)d_p + \left(\frac{1-\varphi_g}{J} \cdot \frac{2}{d_b^2}\right)d_p^2 \tag{23}$$

Interception is relatively independent of flow velocity but increases as bubble diameter decreases, as seen in Eq. 23.

Impaction is the predominant collection mechanism for scrubbers having gas stream velocities greater than 0.3 m/s[35] or for particles whose diameters are larger than 5.0 μm.[36] The Stokes number, Stk, is the dimensionless parameter indicating the impaction effect and is defined as

$$Stk = \frac{\rho_p d_p^2 (u_0 - v_t)}{18\mu d_b} \tag{24}$$

where u_0 is velocity of the tray hole, v_t, the sedimentation velocity of particles, and ρ_p, the particle density.

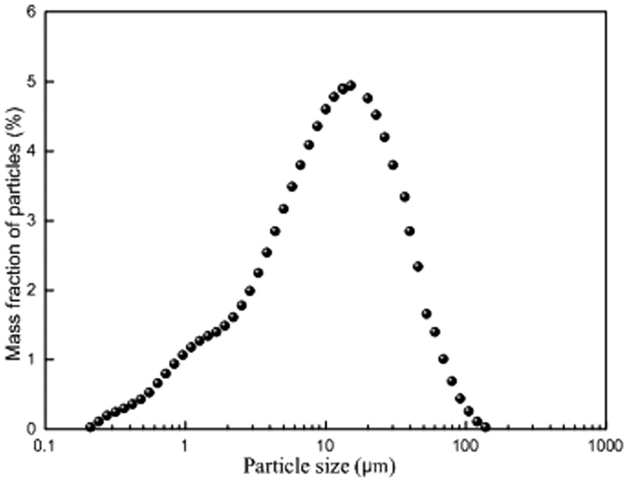

Figure 3. Size distribution of the coal gasification fly-ash particles.

For single bubble, Lee[14] derived the impaction collection efficiency of particles, η_{imp} in bubble scrubber as

$$\eta_{imp}=\left(\frac{Stk}{Stk+0.35}\right)^2 \tag{25}$$

The rate of deposition of particles onto a surface from a region of height h containing n particles per unit volume is[37]

$$-\frac{dn}{dt}=n\frac{v_t}{h} \tag{26}$$

From which the fraction of particles undeposited after time t is

$$\frac{n}{n_0}=\exp\left[\frac{v_t\cdot t}{h}\right] \tag{27}$$

where n_0 is the number of particles per unit volume in the region at time zero

$$\eta_{sed}=1-\frac{n}{n_0}=1-\exp\left[-\frac{v_t\cdot t}{h}\right] \tag{28}$$

In a spherical bubble of radius R_b, it can be shown that the average particle fall distance is[11]

$$h=\frac{\pi}{2}R_b \tag{29}$$

Therefore, the fraction of particles removed by sedimentation during t seconds of residence is

$$\eta_{sed}=1-\exp\left[-\frac{\rho_p g d_p^2 C t}{9\pi R_B \mu_g}\right] \tag{30}$$

The parameters in this calculation have the following values: particle density $\rho_p = 1.85$ g/cm^3 (measured); temperature = 24°C (measured); terminal velocity

$$v_t=\frac{\rho_p g d_p^2 C}{18\mu_g} \tag{31}$$

The overall collection efficiency by a single bubble (η_s) is sum of the above four collection efficiencies, as the collection efficiencies are assumed to be additive by Lim et al.,[38] Sarkar et al.,[39] and Mohan et al.[16] Hence

$$\eta_s=\eta_{diff}+\eta_{inter}+\eta_{sed}+\eta_{imp} \tag{32}$$

Experimental Setup

Materials, apparatus and method

The fly-ash particles used in the study were collected from a OMB gasification system in Linggu, Jiangsu Province, China. The size distribution of fly-ash particles was analyzed by a particulate size analysis system (Model: Mastersizer 2000). The original size distribution of fly-ash particulates is plotted in Figure 3. The sizes of the fly-ash particles ranged from 0.275 to 158.485 μm, close to Gaussian distribution. In addition, the surface morphologies of the fly-ash particulates from scanning electron microscope (SEM) analysis are shown in Figures 4a,b. In Figure 4a, it is evident that the size distribution of the fly-ash particulates was wide. Figure 4b shows one fly-ash particulate with size close to 7 μm. It can be seen that the surface of fly-ash particulates was very smooth and attached tiny powder.

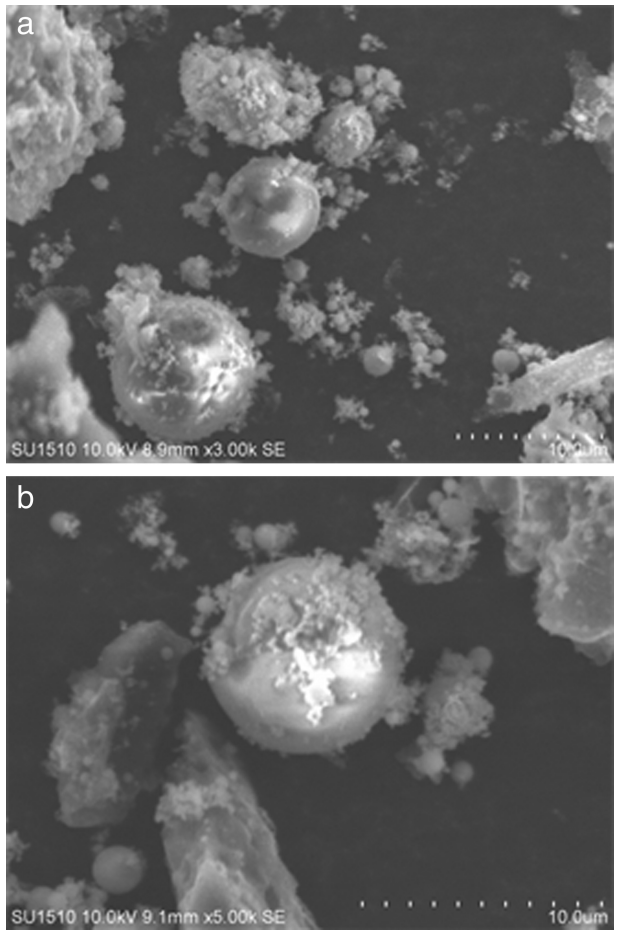

Figure 4. Surface structure of fly-ash particulates with SEM photographs: (a) ×3000 and (b) ×5000.

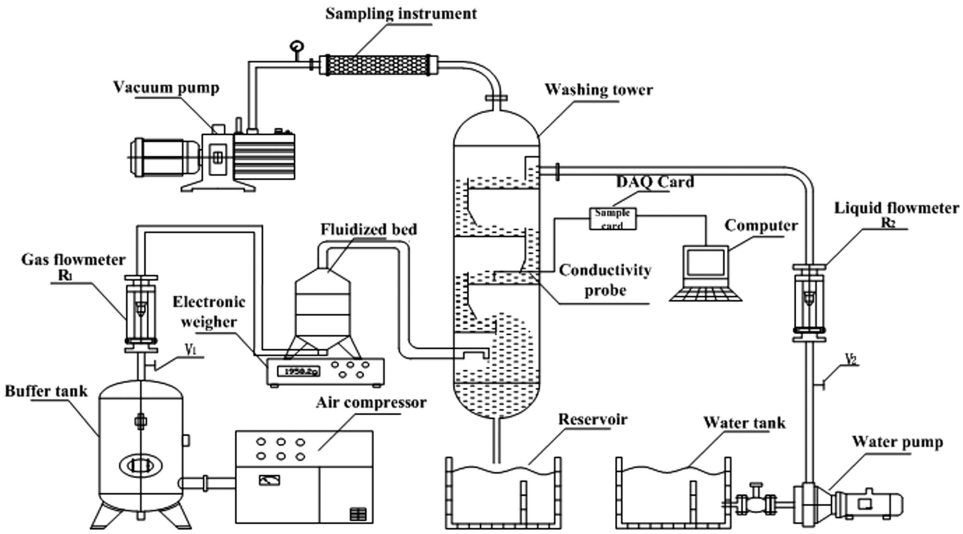

Figure 5. Experiment flow chart.

Figure 5 shows the experimental setup. The experimental bubble scrubber is a vertical cylindrical Perspex column, 90 mm in diameter, and 1350-mm long. The structure of the fixed valve tray is shown in Figure 6. The tray structural parameters are as follows: weir length of 80 mm, weir height of 50 mm, and perforation (the ratio of perforation area to tray area) of 11.8%.The vertical Perspex column has been constructed in three vertical stages, which, in effect, operate in series.

The air–particle mixture was generated by mixing air and particles in a fluidized bed. Compressed air from the compressor was used as the motive fluid in the fluidized bed to blow and thoroughly mix air with particle in fluidized bed, and the mixture was fed into the bottom of the washing column.

In the actual experiment, water was continuously fed at the top of the column through valve and rotameter and withdrawn at the bottom at such a rate that a particular liquid height and bubble volume gas–liquid dispersion volume can be maintained in the column. To collect representative samples, particle samples were withdrawn completely.

The particle concentrations at the top of the scrubber were measured by filtration techniques by passing air borne particles through a glass fiber filter paper (99% or higher efficiency for particles 0.3 μm or larger in diameter) mounted on a filter holder. Samples at this point were drawn under steady-state operating conditions at gas flow rate ranging from 4 to 8 m^3/h to match the experimental gas flow rate. The particles collected on the filter paper were dried at 378 K and cooled in desiccators. The difference in weight of the filter paper containing particles and the filter paper previously weighed alone gave the total mass of particles collected.

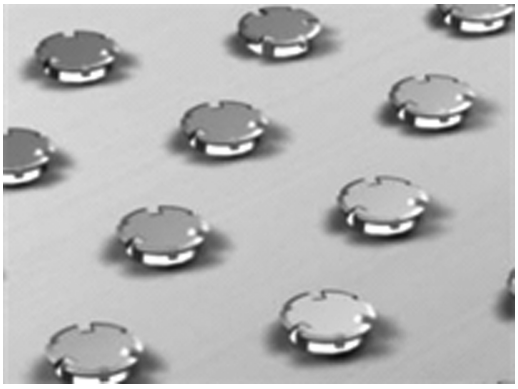

Figure 6. The fixed valve tray.

Experiments have been conducted with liquid flow rates of 160–280 L/h. Corresponding to liquid flow rate, gas flow rates of 4—8 m^3/h were used. The scrubbing liquid in these sets of experiments was water. The collection efficiency of fly-ash has been calculated for each run by the formula as follows:

(1) Overall collection efficiency

The difference in weight of the filter paper containing particles and the filter paper previously weighted alone, gave the total mass of particle collected. The total efficiency of the scrubber in particulate separation, E_T was determined gravimetrically as follows

$$E_T = 1 - \frac{m_{out}}{m_{in}} \tag{33}$$

where m_{out} is mass of unseparated particle in exit air retained on filter (g), m_{in} is mass of particle fed into scrubber (g).

(2) Grade efficiency

The grade efficiency was calculated using the following equation

$$G(x) = 1 - (1 - E_T)\frac{\omega_{out,x}}{\omega_{in,x}} \tag{34}$$

where $\omega_{out,x}$ is mass fraction of unseparated particle in exit air retained on filter at particle size x, and $\omega_{out,x}$ is mass fraction of particle fed into scrubber at particle size x.

Results and Discussion

Gas holdup and collection efficiency

The experimental values of gas holdup are shown in Figure 7. It can be seen from the figure that the gas holdup is gradually increasing with the superficial gas velocity. The data of the present system are also compared with the data reported in the literature[32,40] for gas holdup against superficial gas velocity measured

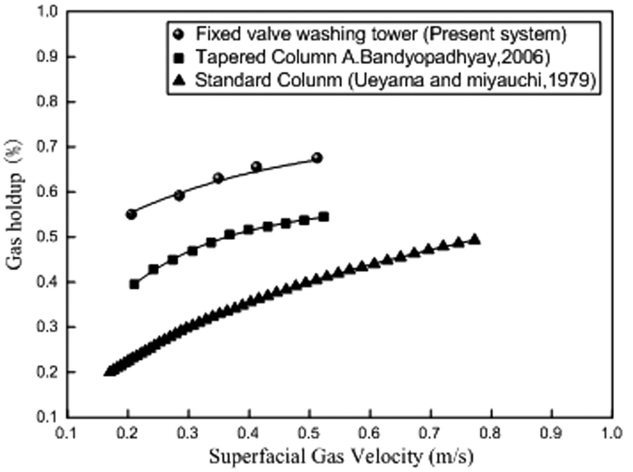

Figure 7. Effect of superficial gas velocity on gas holdup.

for air–water system in standard bubble columns with circular cross-section and tapered column. It shows that the present system offers relatively higher holdup than the existing systems under similar situations. The dependence of the gas holdup on superficial gas velocity in the present system is found to be of the following form[41]

$$\varphi_g = 1 - \exp\left(-0.45 - 0.59\sqrt{F_g}\right) \tag{35}$$

The parameter β can be easily and directly calculated from the experimental values of bubble size using Eq. 12. As illustrated in Figure 8 that β decreases with the increasing F-factor and depends quite weakly on the liquid flow rate.

Although β is the function of C_d, C_n, and We_c, as shown in Eq. 14, C_n and We_c usually behave to be constants, or of small deviations as pointed out in most of the articles.[42] Therefore, the decreasing β with the increasing F_g is attributed to the dependence of C_d on F_g and the regressive expression of β can be obtained as

$$\beta = 0.1175 F_g^{-0.7729} \tag{36}$$

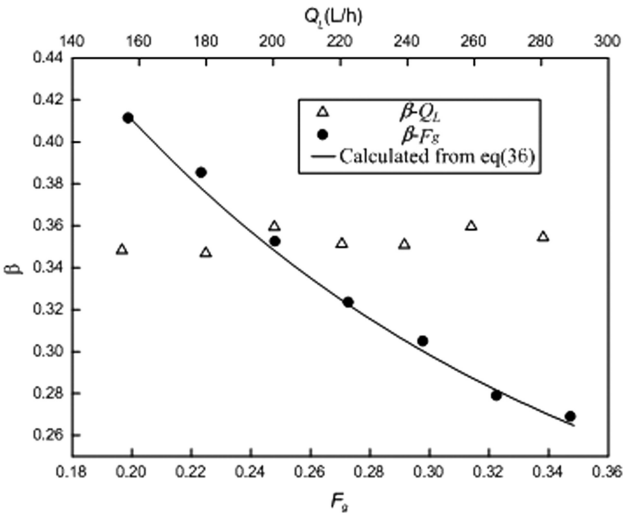

Figure 8. β values as a function of F_g factors and liquid flow rate.

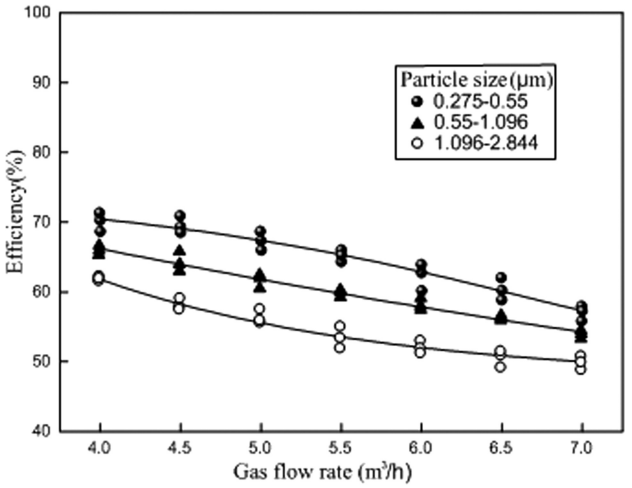

Figure 9. Effect of gas flow rate on collection efficiency of particles finer than 3 μm at constant liquid flow rate.

Combining Eq. 36 with Eq. 13

$$\eta_{total} = 1 - \frac{c}{c_0} = 1 - \exp\left\{-0.42\left(\frac{\sigma}{\rho_L}\right)^{-0.6} \cdot \frac{U}{v_b} \cdot F_g^{-0.373} \cdot H_F \cdot \eta_s\right\} \tag{37}$$

Effect of gas flow rate on collection efficiency

The effect of gas flow rate on collection efficiency of particle is shown in Figures 9 and 10. Each curve in these figures has been obtained for a fixed water flow rate 200 L/h and inlet particle loading 30 g/m^3. Slopes of lines through the points in Figure 9 are negative; slopes in Figure 10 are nearly zero or positive. So that means increasing gas flow rate, the collection efficiency falls down for particles smaller than 3 μm, whereas the collection efficiency increases for particles larger than 5 μm.

For particles finer than 3 μm, the collection efficiency of fly-ash decreases with the increase in gas flow rate. This is because the diffusion mechanism is very much dependent on

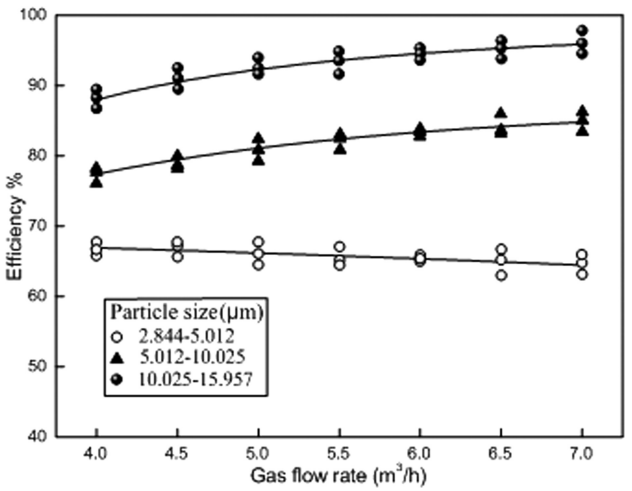

Figure 10. Effect of gas flow rate on collection efficiency of particles lager than 3 μm at constant liquid flow rate.

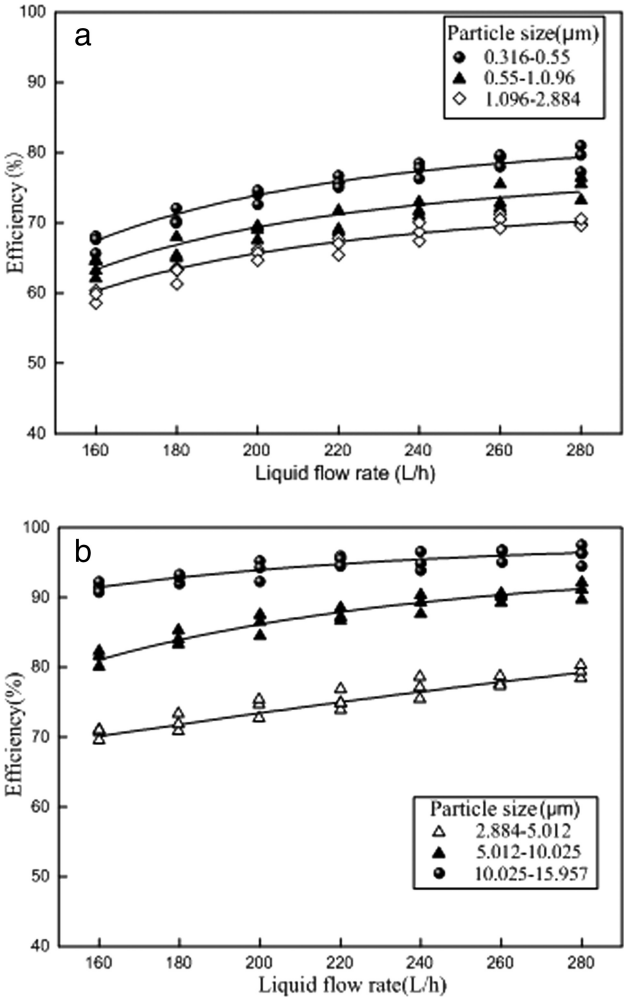

Figure 11. Effect of liquid flow rate on collection efficiency at constant gas flow rate in the fixed valve column (a: 0.3–0.5 μm, 0.5–1 μm, 1–3 μm; b: 3–5 μm, 5–10 μm, 10–15 μm).

residence time and the particle size.[13] As particle size decreases and particle residence time increases, the diffusive mechanism becomes more important. Small particles attain a high diffusion coefficient, because the diffusion coefficient is inversely proportional to size, and the particle residence time increases will enhance the probability of particle–bubble surface collisions in the washing column. Increasing of the inlet air flow rate, results in shorter residence time in the scrubber. Consequently, the removal efficiency will decrease by decreasing the residence time of the particles smaller than 3 μm.

It appears from the Figure 10 that the collection efficiency of fly-ash increases for particles lager than 3 μm with the increase in gas flow rate. As the gas flow rate increases, the gas holdup increases as well as the intensity of bubble bursting, regeneration, and rebursting increases. The particle–bubble interaction would have become a dominant factor in such a situation, which might have contributed positively to higher particle collection. The increase in collection efficiency with the increase in gas flow rate may also attribute to the cyclonic action created by the tangential entry of the air on the plate. With the increased gas flow rate, the fly-ash particles spin outward toward the sidewall of the collecting tube. Thus, at higher gas flow rates, higher particle–bubble interaction, higher gas holdup, and higher cyclonic action might have caused higher collection of fly-ash particles.

Effect of liquid flow rate on collection efficiency

The effect of water flow rate on collection efficiency of particle is shown in Figure 11. Each curve in the figure has been obtained in a fixed gas flow rate 4 m^3/h and inlet particle loading 30 g/m^3. It can be seen from the figure that the collection efficiency of particle increases with the increase of water flow rate. In the present investigation, as the liquid flow rate is increased, the bubble-water interfacial contact area increases.[43] As a result, the collection efficiency increases with the increase in water flow rate. In addition, when enough contact area is available, the particle cut diameter is more dependent on the efficiency of individual collecting surface than that of total collecting surface (number of bubbles).[44] Thus, although the increase of water flow rate may not increase the total number of bubbles, it still affects positively the efficiency of individual bubbles. Increase of collection efficiency might also be due to the faster removal of particles by the downward flowing liquid, which reduces the particle–particle collisions, the re-entrainment of the particles by the bubbles and their release during bubble break up.

Effect of particle size on collection efficiency

The effect of particle size on the removal efficiency is depicted for constant air flow rate 4 m^3/h while using constant water flow rate of 240 L/h and inlet particle loading 30 g/m^3. As shown in Figure 12, by increasing the particle sizes, higher removal efficiency has been obtained. This figure shows that the removal efficiency has a sharp increase by increasing the particle size. Large particles moving toward the liquid have mass, and therefore momentum, which causes each particle to travel in a straight line toward the liquid. The particle leaves the streamline as the streamline bends to move around the liquid. The greater the mass of the particle the more likely that it will travel in a straight line. Also, as the velocity difference between the particle and the liquid increases, the particle will have increased momentum and will be more likely to be carried into the liquid. The radius of curvature of the bend in the streamline has a very important effect on the probability that a particle will be carried into the liquid. The smaller the radius of

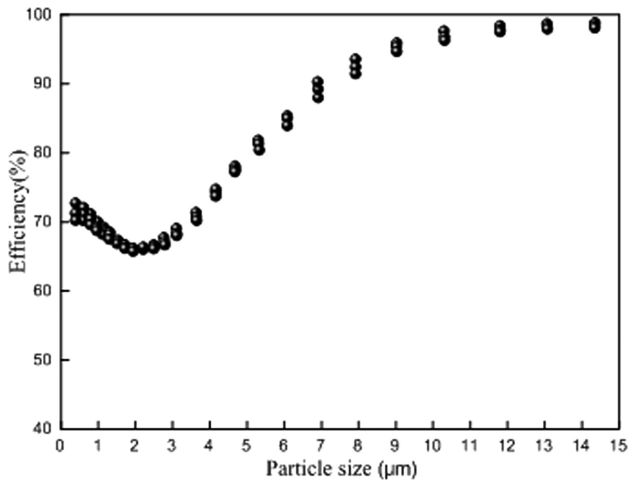

Figure 12. Effect of particle size on collection efficiency at constant liquid and gas flow rate in the fixed valve column.

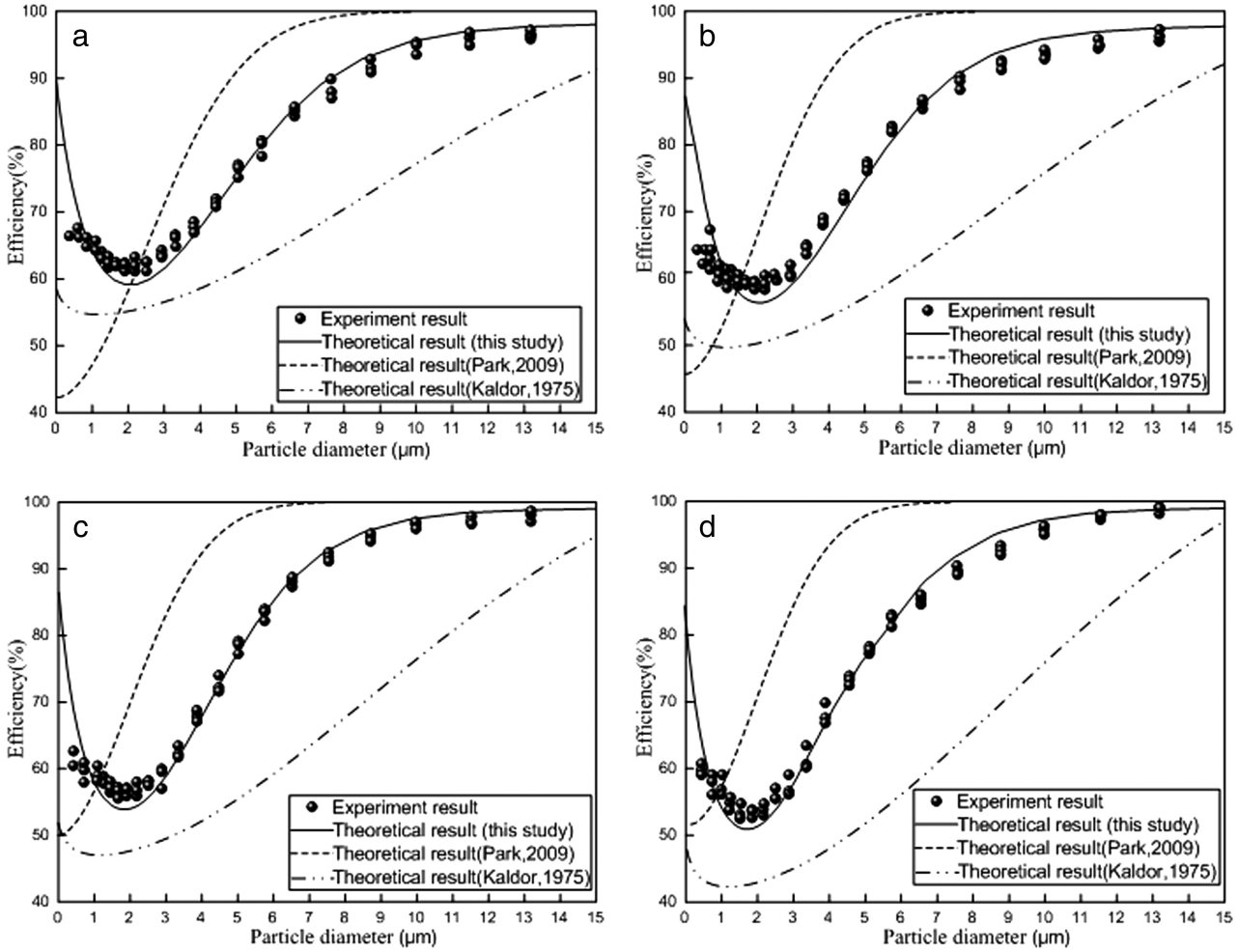

Figure 13. Comparison of the collection efficiency due to scrubbing obtained under four different gas flow rates with the theory (a: gas flow rate 4 m^3/h; b: gas flow rate 5 m^3/h; c: gas flow rate 6 m^3/h; and d: gas flow rate 7 m^3/h).

curvature, the less likely that a particle will follow the streamline.[5] Therefore, small bubbles are more likely to be impacted than large bubbles.

With the particle sizes decreasing, the collection efficiency decreased at first and then increases again. And the minimum value appears among 1 and 3 μm, due to the cross-over from the diffusive to the sedimentation mechanism of particle removal.[11] Particles of roughly 0.3–1 μm diameter are carried by the gas streamline sufficiently close to the surface of the bubble that the particle touches the bubble. These particles have insufficient inertia to leave the gas streamline and are carried with the streamline. Some particle will flow very close to the bubble surface. This mechanism known as interception is a relatively weak mechanism for particle collection compared with impaction. It is coincidental that the path of the streamline and the particle happens to be close to the liquid. It is for this reason that particles in this size range are difficult to collect compared to larger and smaller particles. As indicated in Figure 12, the removal efficiency for particles larger than 15 μm becomes $\sim$100% while using 200 L/h water. These results show the very good performance of this scrubber.

Prediction of particle collection efficiency

The developed mathematical model was calculated for the theoretical collection efficiency. The program was calculated for variable like liquid flow rate, gas flow rate, particle sizes, and the number of trays. The results are plotted, and the values estimated for the parameters in Eqs. 6–34 are presented.

Figures 13a–d represent the calculated results on the effect of particle size on collection efficiency at different gas flow rates, constant liquid flow rate 160L/h, and inlet particle loading 30 g/m^3. The experimentally obtained collection efficiencies were well modeled with foam height H = 0.051–0.083 m and compared with the collection efficiency equation developed by Park[18] and Kaldor.[11] However, their equations were not suitable for predicting collection efficiency in fixed valve tray washing column.

For particle larger than 3 μm, as the particle size increases, the collection efficiency increases steadily and reaches the maximum nearly 100% for particles of 15 μm at gas flow rate of 4 m^3/h and liquid flow rate of 200 L/h. As the particle size increases above 5 μm, the Stokes number in the impaction mechanism and the terminal velocity in the sedimentation mechanism increase obviously.

Figure 14 presents the effect of water flow rate on the theoretical collection efficiency at constant gas flow rate (5 m^3/h). The experimentally obtained collection efficiencies were well modeled with H_F = 0.06 m. As the liquid flow rate increases from 160 to 280 L/h, the overall theoretical collection efficiency also increases markedly.

Figure 15 represents the theoretical efficiency of the valve tray column with respect to the tray number at gas flow rate 4 m^3/h and liquid flow rate 160 L/h. The experimentally obtained collection efficiencies were well modeled with H_F = 0.051–0.132 m. As tray number increases, the overall theoretical efficiency increases markedly. For particle size 1–3 μm, a maximum efficiency of 80% was achieved after three trays for the given gas and liquid flow rate, and the theoretical efficiency was found to increase from 65 to 80% with a steady increase from one tray to three trays in the washing column. The changes occurring in the theoretical efficiency for 1–3 μm were found to be very distinct when compared to other size particles. For the particle larger than 3 μm, the overall theoretical efficiency was found to increase at lower rate due to purification effect of the first plate, the concentration rapidly reduces and the interactions between particles abate. Compared to effect of gas flow rate and liquid flow rate, the effect of the tray number is much significant for the given range of particles.

Conclusions

Particle collection efficiency of a fixed valve tray washing column has been theoretically investigated with a comprehensive analysis of model and experimentally verified for various operating conditions. The theoretical results were compared with the results of other models. The results drawn from this study can be summarized as follows:

1 A mathematical model based on mass balance to a cylindrical element has been developed to predict coal gasification fly-ash collection efficiency.

2 The experimental values of particle removal efficiencies are compared with the theoretically predicted values. It has been found that the particle collection efficiencies are greatly dependent on the particle size, gas flow rate, liquid flow rate, and the tray number.

3 The impaction and gravitational sedimentation of particle collection mechanisms are dominant for particles larger than 5 μm in fixed valve column. For particle lager than 5 μm, as the gas velocity increases, the collection efficiency increases. However, for particle finer than 1 μm, as the gas velocity increases, the collection efficiency decreases due to gas residence time decrease. And the minimum value appears between 1 and 3 μm, due to the cross-over from the diffusive to the sedimentation mechanism of particle removal.

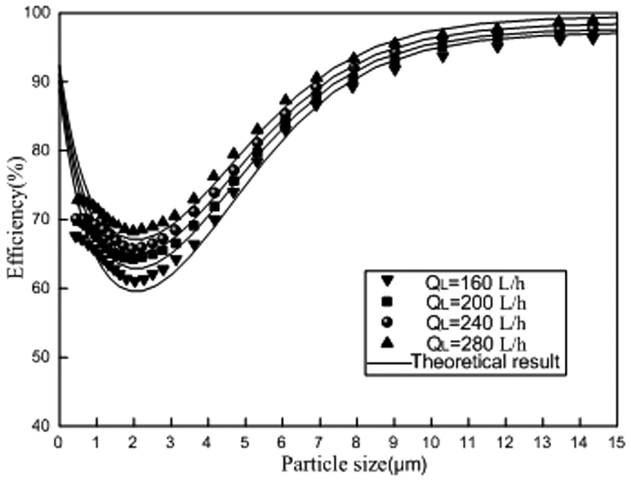

Figure 14. Comparison of the collection efficiency due to scrubbing obtained under four different liquid flow rates with the theory.

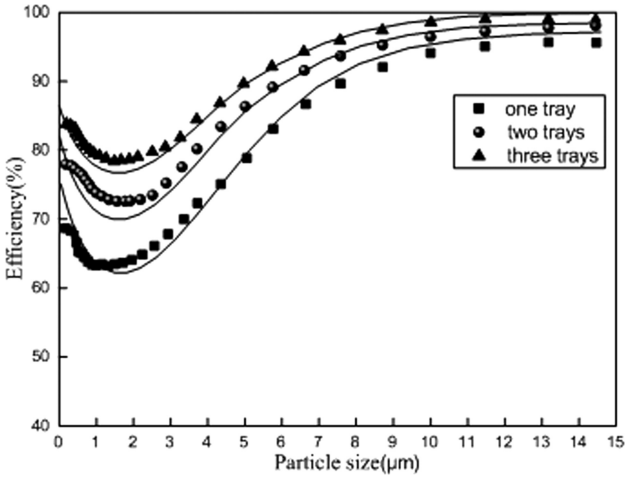

Figure 15. Comparison of the collection efficiency due to scrubbing obtained under different plate number with the theory.

Acknowledgment

The authors are grateful for the financial support from National High-tech R&D Program (2007AA050301).

Notation

A_b = the bubble area of the tray, m^2
A_c = tray bubbling area, m^2
c = particle concentration, g/m^3
C = the Cunningham slip correction factor
d_b = the Sauter bubble mean diameter, m
d_h = the valve diameter
d_{max} = maximum stable bubble diameter, m
d_p = particle Sauter mean diameter, m
D_{diff} = diffusion coefficient, cm^2/s
F_λ = the inertial force of arriving eddy, N
F_σ = the interfacial force, N
h = valve height, m
H_F = froth height, m
H_0 = clear liquid height, m
J = hydrodynamic factor, $J = 1 - \frac{6}{5}\varphi_g^{1/3} + \frac{1}{5}\varphi_g^2$
k = Boltzmann constant, g $cm^2/(s^2\ K)$
k_L = the individual film mass-transfer coefficient
l = the effective valve perimeter
m_{out} = the mass of unseparated particle in exit air retained on filter, g
m_{in} = the mass of particle fed into scrubber, g
n = the number of particles per unit volume
N = bubble number
Q_G = gas flow rate, m^3/s
Q_L = liquid flow rate, m^3/s
Pe = Peclet number, $Pe = \frac{d_b v_b}{D_{diff}}$
R = interception parameter, $R = \frac{d_p}{d_b}$
Stk = Stokes number, $Stk = \frac{\rho_p d_p^2 (u_0 - v_t)}{18 \mu d_b}$
t = time, s
T = absolute temperature, K
u_g = the superficial gas velocity, m/s
u_l = the superficial liquid velocity, m/s
U = the relative velocity between bubbles and liquid, m/s,
v_b = the bubble velocity, m/s
v_0 = the velocity of the hole, m/s
We = Weber number
We_c = the critical Weber number

Greek letters

α = area density, /m
η_{diff} = the fraction of particles collected in a bubble due to diffusion
η_{imp} = the fraction of particles collected in a bubble due to impaction

η_{int} = the fraction of particles collected in a bubble due to interception
η_{sed} = the fraction of particles collected in a bubble due to sedimentation
η_s = the fraction of particle collected in a bubble, $\eta_s = \eta_{diff} + \eta_{inter} + \eta_{sed} + \eta_{imp}$
η_{total} = the overall collection efficiency of washing column
ε = energy dissipation rate per unit liquid mass, m^2/s^3
λ = mean free path length of molecules, cm
σ = surface tension, N/m
φ_g = gas holdup
φ_l = liquid holdup
$\omega_{out,x}$ = mass fraction of unseparated particle in exit at particle size x
$\omega_{in,x}$ = mass fraction of particle fed into scrubber at particle size x
ρ_p = particle density, kg/m^3
ρ_g = gas bubble density, kg/m^3
ρ_l = liquid density, kg/m^3
μ_g = gas viscosity, Pa s
μ_l = liquid viscosity, Pa s

Subscripts

c = critical
diff = diffusion
imp = impaction
int = interception
Max = maximum stable
L = liquid
G = gas
P = particle
Sed = sedimentation

Literature Cited

1. Cui J, Chen X, Gong X, Yu G. Numerical study of gas–solid flow in a radial-inlet structure cyclone separator. *Ind Eng Chem Res*. 2010;49(11):5450–5460.
2. Yoshida H, Ono K, Fukui K. The effect of a new method of fluid flow control on submicron particle classification in gas-cyclones. *Powder Technol*. 2005;149(2):139–147.
3. Wark K, Warner GF, Davis WT. *Particulate Control, Air Pollution: Its Origin and Control*, 3rd ed. Menlo Park, CA: Addison-Wesley, 1998;188–293.
4. Dullien FAL. *Introduction to Industrial Gas Cleaning*. San Diego, CA: Academic Press, 1989;55–90.
5. Schnelle Jr KB, Brown CA. *Air Pollution Control Technology Handbook*. Boca Raton, Fla: CRC Press, 2002;292–294.
6. Lehr F, Millies M, Mewes D. Bubble-size distributions and flow fields in bubble columns. *AIChE J*. 2002;48(11):2426–2443.
7. Martín M, García JM, Montes FJ, Galán MA. On the effect of the orifice configuration on the coalescence of growing bubbles. *Chem Eng Process: Process Intens*. 2008;47(9–10):1799–1809.
8. Meikap BC, Kundu G, Biswas MN. Scrubbing of fly-ash laden SO_2 in modified multistage bubble column scrubber. *AIChE J*. 2004;48(9):2074–2083.
9. Morton WE, Fairbanks HV, Wallis J, Hunicke RL, Krenicki J. Ultrasonic vibrator tray apparatus. US Patent 4,919,807 (1990)
10. Levy EK, Parkinson JW, Arnold B, Salmento J. Fly ash processing using inclined fluidized bed and sound wave agitation. US Patent 5,996,808 (1990)
11. Kaldor TG, Phillips CR. Aerosol scrubbing by foam. *Ind Eng Chem Process Des Dev*. 1976;15(1):199–206.
12. Clair HWS. Agglomeration of smoke, fog, or dust particles by sonic waves. *Ind Eng Chem*. 1949;41(11):2434–2438.
13. Fuchs NA. *The Mechanics of Aerosols*. New York: Pergamon Press, 1964.
14. Lee KW, Gieseke JA. Collection of aerosol particles by packed beds. *Environ Sci Technol*. 1979;13(4):466–470.
15. Jung C, Lee K. Filtration of fine particles by multiple liquid droplet and gas bubble systems. *Aerosol Sci Technol*. 1998;29(5):389–401.
16. Raj Mohan B, Jainb RK, Meikap BC. Comprehensive analysis for prediction of dust removal efficiency using twin-fluid atomization in a spray scrubber. *Sep Purif Technol*. 2008;63(2):269–277.
17. Lee B, Jung K, Park S. Development and application of a novel swirl cyclone scrubber-(1) Experimental. *J Aerosol Sci*. 2008;39(12):1079–1088.
18. Park S-H, Lee B-K. Development and application of a novel swirl cyclone scrubber (2) Theoretical. *J Hazard Mater*. 2009;164(1):315–321.
19. Kemoun A, Rados N, Lia F, Al-Dahhana MH, Dudukovića MP, Millsb PL, Leibc TM, Leroud JJ. Gas holdup in a trayed cold-flow bubble column. *Chem Eng Sci*. 2001;56(3):1197–1205.
20. Jaćimović B, Genić SB. Froth porosity and clear liquid height in trayed columns. *Chem Eng Technol*. 2000;23(2):171–176.
21. Kolmogoroff AN. On the breaking of drops in turbulent flow. *Dokl Akad Nauk SSSR*. 1949;66:825–828.
22. Hinze JO. Fundamentals of the hydrodynamic mechanism of splitting in dispersion processes. *AIChE J*. 1955;1(3):289–295.
23. Levich VG. Spalding DB. *Physicochemical Hydrodynamics*. Englewood Cliffs, NJ: Prentice-Hall, 1962:87–88.
24. Sevik M, Park S. The splitting of drops and bubbles by turbulent fluid flow. *J Fluids Eng*. 1973;95:53–60.
25. Hesketh RP, Russell TWF. Bubble size in horizontal pipelines. *AIChE J*. 1987;33(4):663–667.
26. Wilkinson PM, Van Schayk A, Josette PM. The influence of gas density and liquid properties on bubble breakup. *Chem Eng Sci*. 1993;48(7):1213–1226.
27. Martinez-Bazan C, Montanes JL, Lasheras JC. On the breakup of an air bubble injected into a fully developed turbulent flow. Part 1. Breakup frequency. *J Fluid Mech*. 1999;401:157–182.
28. Martinez-Bazan C, Montanes JL, Lasheras JC. On the breakup of an air bubble injected into a fully developed turbulent flow. Part 2. Size PDF of the resulting daughter bubbles. *J Fluid Mech*. 1999;401:183–207.
29. Risso F. The mechanisms of deformation and breakup of drops and bubbles. *Multiphase Sci Technol*. 2000;12(1):1–50.
30. Batchelor G. *Theory of Homogeneous Turbulence*. Cambridge: Cambridge University Press, 1982:34.
31. Liang YC, Zhou Z, Shao M, Geng J, Wu Y-T, Zhang Z-B. The impact of valve tray geometry on the interfacial area of mass transfer. *AIChE J*. 2008;54(6):1470–1477.
32. Bandyopadhyay A, Biswas MN. Fly-ash scrubbing in a tapered bubble column scrubber. *Process Saf Environ Prot*. 2006;84(1):54–62.
33. Friedlander SK. *Smoke, Dust and Haze: Fundamentals of Aerosol Behavior*, 1st ed. New York: Wiley-Interscience, 1977:333.
34. Allen MD, Raabe OG. Slip correction measurements of spherical solid aerosol particles in an improved Millikan apparatus. *Aerosol Sci Technol*. 1985;4(3):269–286.
35. Cheng L. Collection of airborne dust by water sprays. *Ind Eng Chem Process Des Dev*. 1973;12(3):221–225.
36. Kim HT, Jung CH, Oh SN, Lee KW. Particle removal efficiency of gravitational wet scrubber considering diffusion, interception, and impaction. *Environ Eng Sci*. 2001;18(2):125–136.
37. Green HL, Lane WR. *Particle Clouds, Dusts, Smokes and Mists*. London: E. and F. N. Spon, Ltd., 1957.
38. Lim KS, Lee SH, Park HS. Prediction for particle removal efficiency of a reverse jet scrubber. *J Aerosol Sci*. 2006;37(12):1826–1839.
39. Sarkar S, Meikap BC, Chatterjee SG. Modeling of removal of sulfur dioxide from flue gases in a horizontal cocurrent gas–liquid scrubber. *Chem Eng J*. 2007;131(1):263–271.
40. Shah YT, Kelkar BG, Godbole SP, Deckwer W-D. Design parameters estimations for bubble column reactors. *AIChE J*. 1982;28(3):353–379.
41. AIChE. *Bubble-Tray Design Manual*. New York: AIChE, 1958.
42. Rigby GD, Evans GM, Jameson GJ. Bubble breakup from ventilated cavities in multiphase reactors. *Chem Eng Sci*. 1997;52(21):3677–3684.
43. Meikap BC, Kundu G, Biswas MN. Prediction of the interfacial area of contact in a variable area multi-stage bubble column. *Ind Eng Chem Res*. 2001;40(26):6194–6200.
44. Cooper DW. Theoretical comparison of efficiency and power for single-stage and multiple-stage particulate scrubbing. *Atmos Environ*. 1967;10(11):1001–1004.

Manuscript received Jun. 25, 2012, revision received Sept. 3, 2012, and final revision received Nov. 6, 2012.